Revista de Chimie
https://revistadechimie.ro
https://doi.org/10.37358/Rev.Chim.1949

Thermodynamic and Kinetic Study on the Catalysis of Isobornyl Acetate by a Cation Exchange Resin an Intensified Fixed-Bed Reactor

WANGLAI DONG, LEI CHEN, HANZHAO YAN, ZIJIE ZHANG, ZHENG ZHOU*
School of Chemistry and Chemical Engineering, Nanjing University, 210023 Nanjing, China

Abstract: *Esterification Thermodynamic and Kinetic on acetic acid with camphene was studied systematically in an intensified fixed bed reactor at 303-323 K with anhydrous NKC-9 resin. The catalyst loading, initial molar ratio, temperature, and catalyst reusability were studied and optimized. The method of UNIFAC was applied to calculate the activity coefficient of each component for correcting the nonideality of the solution. Reaction enthalpy, entropy, and Gibbs free energy were calculated. The kinetics of camphene esterification was studied by pseudo-homogeneous model (PH model), and the fitting effect was good, which provided experimental reference and theoretical basis for the industrial production of isobornyl acetate.*

Keywords: *esterification，cation exchange resin，thermodynamics, kinetics*

1.Introduction

Isobornyl acetate, commonly known as leguminous ester, has a fresh woody and camphor fragrance. As a raw material for flavors and synthetic flavors, it is widely used in indoor air fresheners and other daily chemicals, pharmaceutical intermediates, solvents and lubricants synthesis of agent. Isobornyl acetate can be synthesized by esterification reaction of camphene and acetic acid. The reaction mechanism is shown in Figure 1. First, camphene forms an intermediate form of carbon ions under the contact catalysis of acid catalysts, and then quickly rearranges. The rearranged carbocations undergo dehydrogenation with the reaction of acetic acid molecules to form isobornyl acetate. In this reaction, the choice of catalyst is crucial. Gu Y C et al. [1] discussed the effects of catalyst sulfuric acid dosage, reaction time, reaction temperature and other factors on the esterification of low-grade fatty acids C1~C5 with camphene. The related conclusions obtained are that the molar ratio of carboxylic acid to camphene was 1.2:1, the sulfuric acid dosage was 20% of camphene mass, and the reaction is carried out at 15℃ for 3 hours. The yields of several carboxylic acids and camphene were similar. Ivo j. Dijs et al. [2] used three kinds of sulfonated crosslinked polystyrene resin (Dowex 50WX8, Amberlyst 15 and Purolite MN500) as catalysts to catalyze the reaction between acetic acid and camphene, using p-toluenesulfonic acid monohydrate homogeneous the catalyst was investigated by comparative experiments. The experiment found that Amberlyst 15 and Purolite MN500 have a reaction rate similar to that of a homogeneous catalyst, and the catalytic effect is better. This is due to the rigid porous structure of the catalyst, while Dowex 50WX8 is catalyzed by the low degree of crosslinking of the sulfonic acid group. The effect is poor. Ma W L [3] used cationic exchange resin D72 as catalyst to optimize the synthesis of isobornyl acetate in a stirring kettle and a fixed bed reactor. The results showed that the fixed bed had higher catalyst utilization rate and continuous production. Augusto L.P et al. [4] used $H_3PW_{12}O_{40}$(PW) solid acid catalyst supported by silicon dioxide for esterification of camphene and short-chain fatty acids. The reaction conditions were mild and the yield was between 80% and 90%. Yang Y X et al. [5] prepared solid acid catalyst with phosphotungstate supported by SO_4^{2-}/TiO_2 to catalyze the reaction of camphene and acetic acid. After the optimization of experimental conditions, the conversion rate reached 85.5% and the purity of the product reached over 95% after distillation. Cui J T et al. [6] used Lewis acid as catalyst, and through catalyst screening and process parameter optimization, $FeCl_3$ has the best catalytic effect, and the conversion rate of camphene is close to 99%.

email: zhouzheng@nju.edu.cn

Liquid acid has been phased out due to its strong corrosiveness, difficulty in post-treatment, strict production conditions, and serious environmental pollution. Although the solid super acid is easy to separate after the catalytic reaction is completed, the regeneration and recycling of the catalyst is a problem that is difficult to solve in industrial applications. Based on the above problems, in recent years, cation exchange resins have been widely used due to their good chemical stability, easy separation and recovery, safety and pollution-free, high catalytic activity and selectivity [7-12].

In addition, in the choice of reactor, an intensified fixed bed reactor (IFBR), improved from the traditional fixed bed reactor by our research group [13], was applied to conduct esterification reactions of camphene with acetic acid in the existence of anhydrous NKC-9 resin. Compared with the stirred tank reactor, a fixed-bed reactor can effectively solve the mechanical wear problem of the solid catalyst and greatly simplify the process of catalyst recovery and utilization. Compared with the traditional fixed bed reactor, driven by a circulating pump, the liquid passes through the catalyst bed at high speed, which solves the problem that channel flow is easily formed in a conventional fixed-bed reactor due to its slow velocity. Previous studies have shown that the mass transfer coefficient in the IFBR can generally be increased by more than 30% compared with traditional reactors, and the mass transfer area between liquid phases can be more than double [13].

This paper mainly studied the effect of cation exchange resin NKC-9 on the esterification reaction of camphene and acetic acid in the IFBR device. Based on the optimized experimental conditions, the reaction thermodynamics and kinetics were calculated, and the corresponding Thermodynamic and kinetic parameters provide a theoretical basis for industrialized production.

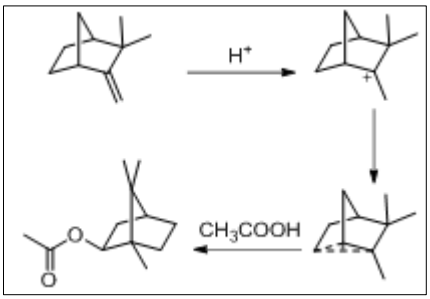

Figure 1. Reaction scheme for the esterification of camphene

2.Materials and methods

2.1 experiment reagent

Camphene (≥93%), Xiamen Zhongkun Chemical Co. LTD, Ice Acetic Acid (> 99%), Alighting Chemical Co. LTD, NKC-9, Tianjin Bohong Resin Technology Co. LTD, Acetone (analyte pure), Nanjing Chemical Reagent Co. LTD. deionized water.

2.2 Experimental apparatus

The reactions were conducted in the IFBR shown in Figure 2, which was equipped with a 250 mL preheating tank, a heating medium circulator (298−373 K), a peristaltic pump (<720 mL/min), and a stainless steel fixed bed. The preheating tank and fixed bed reactor were specially made and both equipped with the corresponding material for the water bath. The peristaltic pump was obtained from Baoding Lead Fluid Technology Co., LTD, for precise control of raw material flow. The heating medium circulator was equipped with a circulating pump to deliver heat flow to the preheating tank and fixed bed.

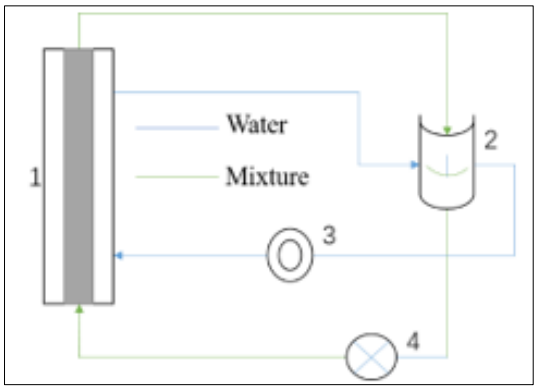

Figure 2. IFBR diagram
(1.fixed bed reactor 2.preheating tank
3.heating medium circulator 4.peristaltic pump)

2.3 Gas chromatographic analysis conditions

The samples were analyzed by Shimadzu GC-2014C chromatography. The gas chromatography conditions are as follows: The chromatographic column is a WondaCap-5c capillary column (30m x 0.32mm x 0.25μm), using an FID detector, the carrier gas is N_2, the pre-column pressure: 45.2kPa; the flow rate of makeup gas (N_2): 30 mL/ min; H_2: 40 mL/min; air: 400 mL/min. The temperature of the chromatographic column was increased by program: the initial temperature was 90°C and kept for 2min; then it was increased to 230°C at a rate of 20°C/min and kept for 10min. The gasification chamber temperature is 290°C, and the detector temperature is 280°C. The injection volume was 0.2μL, and the area normalization method was used for quantitative analysis.

3.Results and discussions

3.1 The influence of the amount of catalyst

Anhydrous NKC-9 was used as the catalyst, the reaction temperature was 303K, and the initial molar ratio of the materials was camphene: acetic acid = 1:3. The effect of the amount of catalyst on the esterification reaction of camphene was explored. The results are shown in Figure 3. Figure 3 (a) clearly shows that conversion of camphene increases from 92.1% to 97.0% with catalyst loading from 5 to 15 wt % at 90 min. while that the conversion of camphene is around 97.0% with catalyst loading from 15 to 25 wt %. This is because the mechanism of the esterification reaction of camphene with acetic acid is a carbanion reaction mechanism, and the more the amount of catalyst is, The more acidic active sites the catalyst can provide, and the higher the concentration of carbanion produced per unit time, so the conversion rate of camphene in the same time is also increased. However, the increase in the amount of catalyst will lead to a decrease in the selectivity of the reaction and more by-products. When the amount of catalyst exceeds 15%, it can be seen that the selectivity of the reaction target product decreases significantly, as shown in Figure 3 (b). Therefore, it is more appropriate to choose 15% for the catalyst amount in this and subsequent reactions.

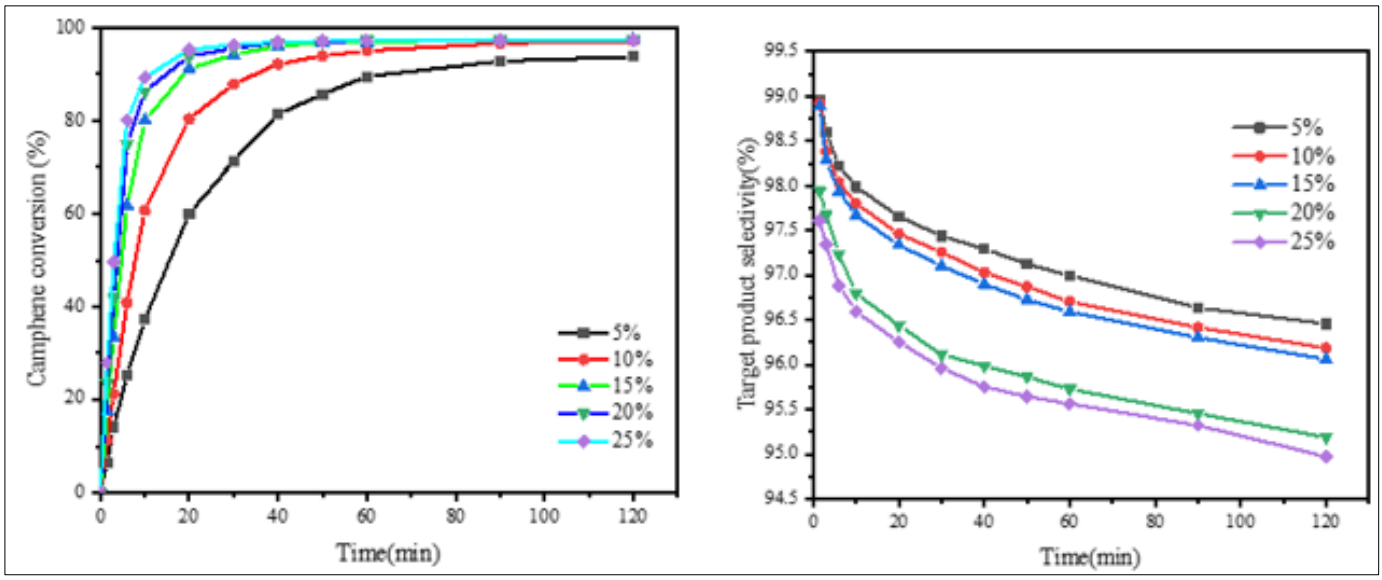

Figure 3. The effect of the amount of catalyst on the esterification of camphene (temperature: 303K; Catalyst: NKC-9; initial molar ratio of materials: camphene: acetic acid =1:3).
(a) The effect of the amount of catalyst on the conversion of camphene, **(b)** The influence of the amount of catalyst on the selectivity of the target product

3.2 The influence of material ratio

Anhydrous NKC-9 was used as the catalyst, the catalyst dosage was 15 wt%, and the reaction temperature was 303K. The effect of the ratio of the amount of camphene and acetic acid on the esterification of camphene was investigated. The results are shown in Figure 4. Shown. Figure (a) shows that when the ratio of the amount of camphene to acetic acid increases from 1:1.2 to 1:3, the conversion rate of camphene rises from 89.6% to 97.3%, but when the ratio of the amount of substances increases from 1:2 to 1:3, the conversion rate of camphene per unit time increases little, just rises from 96.2% to 97.3%, indicating that the increase in the amount of acetic acid at this time has a relatively small effect on the reaction. When the ratio increases from 1:1.2 to 1:3, the selectivity of the target product gradually increases, as shown in Figure (b). Taking into account the economic requirements of the process, when the amount of acetic acid is excessive, continuing to increase the amount of acetic acid will increase the consumption of materials and the energy consumption in the operation of the separated products. Therefore, the ratio of camphene to acetic acid is preferably 1:1.5.

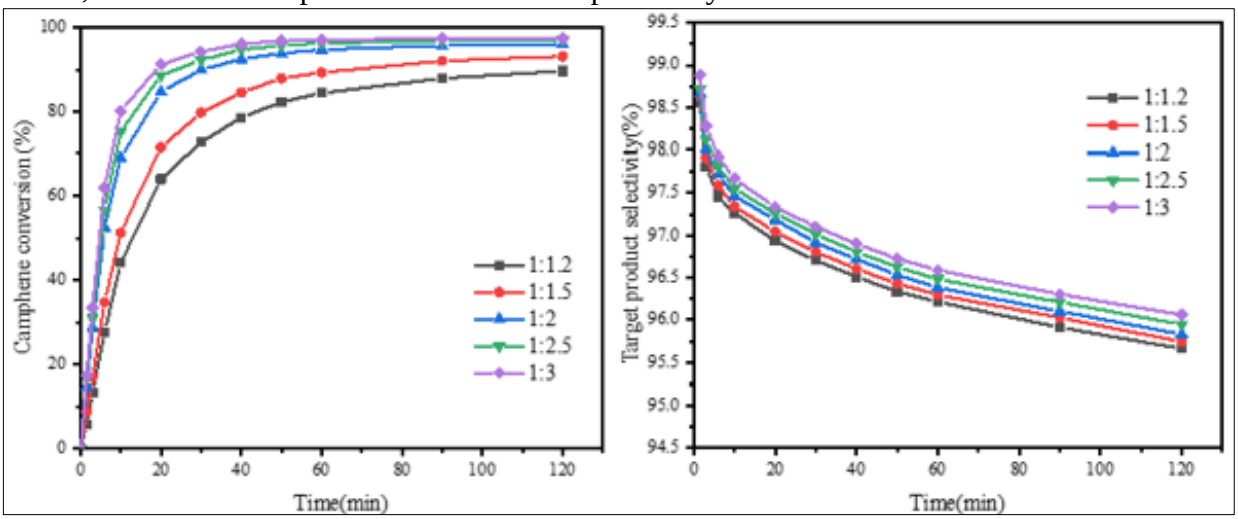

Figure 4. The effect of material ratio on the esterification of camphene (temperature: 303K Catalyst: NKC-9; Catalyst loading: 15% (w/w)). **(a)**The effect of material ratio on camphene conversion**, (b)** The influence of material ratio on target product selectivity

3.3 Effect of reaction temperature

Anhydrous NKC-9 is used as the catalyst, the amount of catalyst is 15 wt%, the initial molar ratio of materials is camphene: acetic acid = 1:1.5. The effect of temperature on the esterification of camphene is explored, and the result is shown in Figure 5. Shown. Figure (a) shows that as the temperature increases from 303K to 323K, the rate of esterification of camphene increases. We found that when the catalytic temperature of the reaction is greater than 308K, its catalytic activity is significantly higher than that at low temperatures (temperature less than 308K) Catalytic activity. However, as the temperature increases, as shown in Figure (b), the selectivity of the target product decreases, and with the extension of the reaction time, the selectivity of the target product also decreases, indicating that the increase in temperature is likely to increase the isomerization of camphene, The resulting product isobornyl acetate will also be isomerized into other products. It can also be seen from Table 1 that when the temperature is high, the yield of the target product decreases, and the lower the temperature, the higher the yield of the target product. Therefore, the comprehensive reaction time, camphene conversion rate, and reaction product yield are selected 308K as the reaction temperature.

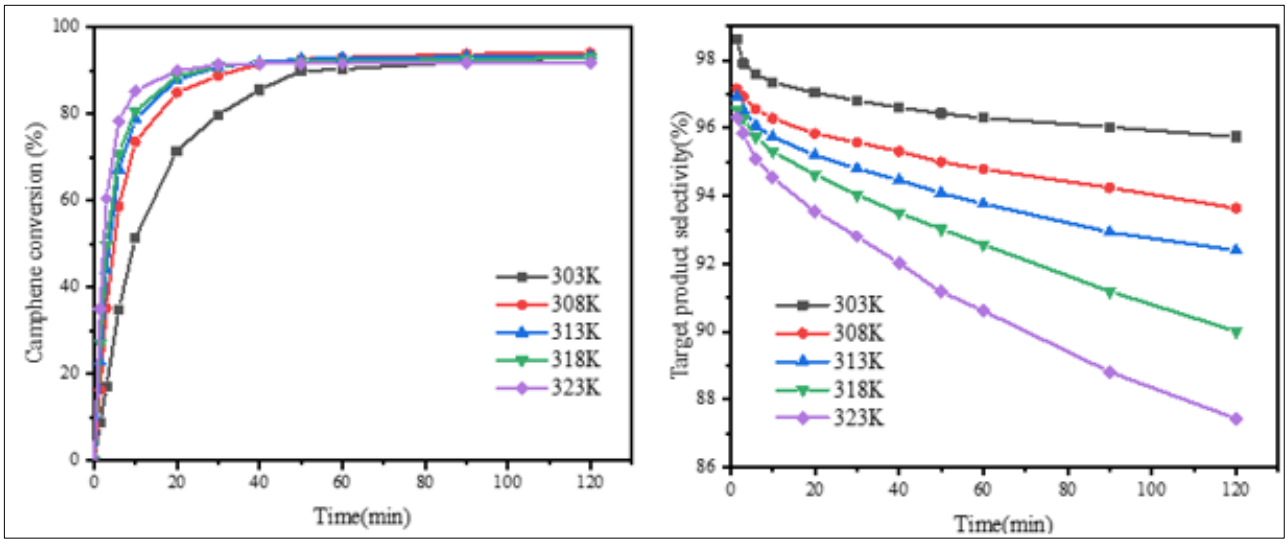

Figure 5. Effect of temperature on the esterification camphene (catalyst: NKC-9; Catalyst loading: 15% (w/w); initial molar ratio of materials: camphene: acetic acid =1:1.5). **(a)** The effect of reaction temperature on camphene conversion**,** **(b)** The effect of reaction temperature on the selectivity of the target product

Table 1. Yield of camphene esterification product at different temperature

T/K Time/min	303K	308K	313K	318K	323K
10	49.907	70.856	75.418	76.859	80.685
20	69.376	81.373	83.746	83.890	84.172
30	77.226	84.932	86.152	85.627	84.768
40	82.650	87.235	86.777	85.672	84.334
50	86.707	88.049	87.164	85.550	83.581
60	86.962	88.202	87.173	85.287	83.034
90	88.420	88.428	86.603	84.385	81.564
120	89.184	88.127	86.282	83.635	80.343

3.4 Reusability of Catalysts

The reusability of the NKC-9 resin in the optimal reaction conditions was investigated in the IFBR. The experimental results showed that the conversion after 20 h hardly changed after the catalyst was recycled 10 times (Figure 6). The SEM results also showed that the resin had almost no wear after 10 repetitions in the IFBR (Figure 7). In summary, the NKC-9 resin showed stable activity in the synthesis

of isobornyl acetate catalysis in the IFBR, which has certain practical application significance and potential industrial use.

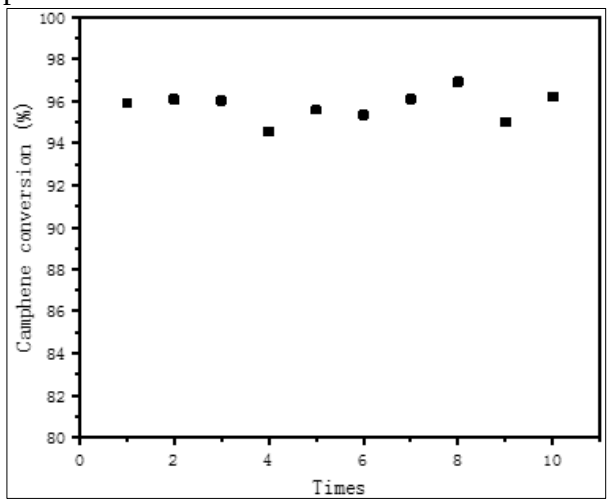

Figure 6. The performance of NKC-9 used repeatedly in IFBR (temperature: 308K; Catalyst loading: 15% (w/w) initial molar ratio of materials: camphene: acetic acid =1:1.5)

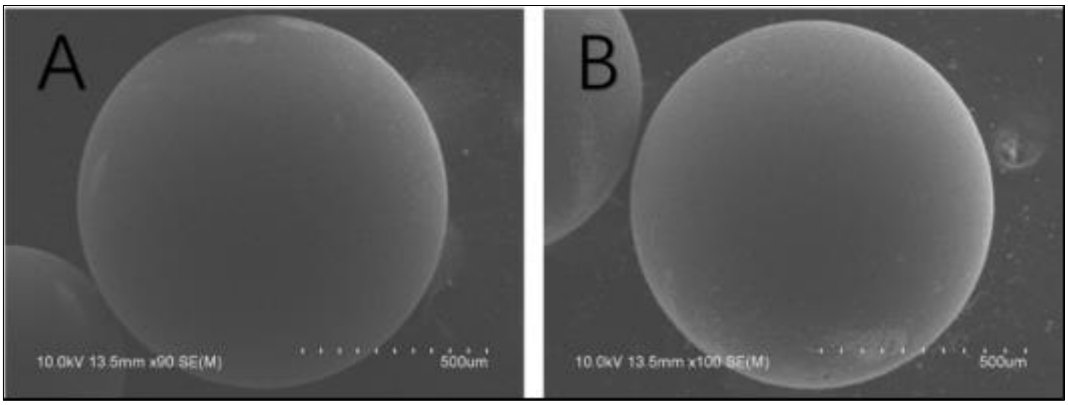

Figure 7. SEM of unused (A) and 10-time used (B) NKC-9

3.5 Thermodynamic calculation

The reaction system of camphene and acetic acid is not ideal, and the interaction between the components must be considered. In order to correct the non-ideality of the solution, the activity is used instead of the concentration to calculate the equilibrium constant of the reaction, and the activity coefficient is estimated by the UNIFAC group contribution method [14,15]. The UNIFAC group contribution method regards the solution as a mixture of groups, and links the activity coefficient of each component in the mixture with the group parameters of the groups constituting the molecules of the mixture, and uses limited group parameters Instead of solutions composed of countless compounds, in this way, for unknown solutions, the activity coefficient can still be reasonably estimated.

The UNIFAC group contribution method divides the activity coefficient of the component into the combined part and the remaining part:

$$\ln\gamma_i = ln{\gamma_i}^{(c)} + ln{\gamma_i}^{(R)} \quad (1)$$

Among them, $\ln\gamma_i^{(c)}$ reflects the combination of molecular size and shape, and, $\ln\gamma_i^{(R)}$ reflects the mutual influence between the remaining groups.

In the formula, the combined term formula is:

$$\ln{\gamma_i}^{(c)} = \ln\frac{\phi_i}{x_i} + \frac{z}{2}q_i ln\frac{\theta_i}{\phi_i} + l_i - \frac{\phi_i}{x_i}\sum_j x_j l_j \quad (2)$$

In the formula, the coordination number z=10:

$$l_i = \frac{z}{2}(r_i - q_i) - (r_i - 1) \quad (3)$$

$$\theta_i = \frac{x_i q_i}{\sum_j x_j q_j} \quad (4)$$

$$\phi_i = \frac{x_i r_i}{\sum_j x_j r_j} \quad (5)$$

$$r_i = \sum_k v_k^{(i)} R_k \quad (6)$$

$$q_i = \sum_k v_k^{(i)} Q_k \quad (7)$$

In the formula, the remaining term formula is:

$$\ln\gamma_i^{(R)} = \sum_k v_k^{(i)} [\ln\Gamma_k - \ln\Gamma_k^{(i)}] \quad (8)$$

$$\ln\Gamma_k = Q_k[1 - \ln(\sum_m \hat{\theta}_m \Psi_{mn}) - \sum \frac{\hat{\theta}_m \Psi_{mn}}{\hat{\theta}_n \Psi_{mn}}] \quad (9)$$

$$\ln\Gamma_k^{(i)} = Q_k[1 - \ln\left(\sum_m \hat{\theta}_m^{(i)} \Psi_{mn}\right) - \sum \frac{\hat{\theta}_m^{(i)} \Psi_{mn}}{\hat{\theta}_m^{(i)} \Psi_{mn}}] \quad (10)$$

$$\hat{\theta}_m = \frac{Q_m \hat{X}_m}{\sum_n Q_n \hat{X}_m} \quad (11)$$

$$\hat{\theta}_m^{(i)} = \frac{Q_m \hat{X}_m^{(i)}}{\sum_n Q_n \hat{X}_n^{(i)}} \quad (12)$$

$$\hat{X}_m = \frac{\sum_i v_m^{(i)} x_{(i)}}{\sum_i \sum_k v_k^{(i)} x_i} \quad (13)$$

$$\hat{X}_m^{(i)} = \frac{v_m^{(i)}}{\sum_k v_k^{(i)}} \quad (14)$$

$$\Psi_{mn} = \exp(-\frac{a_{mn}}{T}) \quad (15)$$

Ψ_{mn} is determined by the interaction parameter a_{mn} of the m-type group and the n-type group. The interaction parameter a_{mn} can be found in the book "Physical Property Estimation Principles and Computer Calculations".

The expression of the chemical equilibrium constant expressed with activity instead of concentration is:

$$\mathrm{K} = \prod a_i^{v_i} = \frac{a_{IA}}{a_{Cam} a_{IA}} = \left(\frac{x_{IA}}{x_{Cam} x_{AA}}\right)\left(\frac{\gamma_{IA}}{\gamma_{Cam}\gamma_{AA}}\right) = K_x K_\gamma \quad (16)$$

UNIFAC group volume parameter, group area parameter and group interaction parameter a_{mn} are shown in Table 2 and Table 3. According to formula (16), the activity coefficients and equilibrium constants of different components at different temperatures are calculated, as shown in Table 4. Show.

Table 2. UNIFAC group volume parameters and group area parameters

Component	Group classification			V_k	Volume parameter	Area parameter
	Group name	Main group	Sub groups		R_k	Q_k
Cam	CH_3	1	1	2	0.9011	0.848
	CH_2	1	2	3	0.6744	0.540
	CH	1	3	2	0.4469	0.228
	C	1	4	1	0.2195	0
	CH_2=C	2	7	1	1.1173	0.988
AA	CH_3	1	1	1	0.9011	0.848
	COOH	20	43	1	1.3013	1.224
IA	CH_3	1	1	3	0.9011	0.848
	CH_2	1	2	3	0.6744	0.540
	CH	1	3	2	0.4469	0.228
	C	1	4	2	0.2195	0
	CH_3COO	11	22	1	1.9031	1.728

Table 3. The interaction parameters of the groups(a_{mn})

n / m		1	2	11	20
		CH_2	C=C	CCOO	COOH
1	CH_2	0	86.02	232.1	663.5
2	C=C	-35.36	0	37.85	318.9
11	CCOO	114.8	132.1	0	660.2
20	COOH	315.3	1264	-256.3	0

Table 4. Activity coefficients and equilibrium constants of different components

T/K	303	308	313	318	323
γ_{Cam}	2.095	2.073	2.053	2.033	2.015
γ_{AA}	0.245	0.247	0.250	0.252	0.255
γ_{IA}	1.526	1.515	1.504	1.493	1.482
K	180.754	148.177	122.087	103.646	87.236

According to the Vanter Hoff equation and the Gibbs free energy calculation formula, the relationship between the equilibrium constant of the reaction and the thermodynamic parameters can be expressed as:

$$\Delta_r G^0 = \Delta_r H^0 - T\Delta_r S^0 \quad (17)$$

$$\ln K = -\frac{\Delta_r G^0}{RT} = -\frac{\Delta_r H^0}{RT} + \frac{\Delta_r S^0}{R} \quad (18)$$

It can be seen that there is a linear relationship between ln K and 1/T, and $\Delta_r H^0$ and $\Delta_r S^0$ can be obtained from the linear slope and intercept. When the temperature is known, the Gibbs free energy can be obtained. Plot lnK versus 1/T, as shown in Figure 8. According to the slope and intercept of the image, the enthalpy change $\Delta_r H^0$ is-29.54kJ/mol, and the entropy change $\Delta_r S^0$ is -54.35J/(mol·K) .According to the Gibbs free energy formula (17), the Gibbs free energy $\Delta_r G^0$ is -13.55kJ/mol, so the chemical equilibrium constant expression for the reaction of camphene and acetic acid can be expressed as:

$$K = \exp\left(\frac{3553.477}{T} - 6.537\right)$$

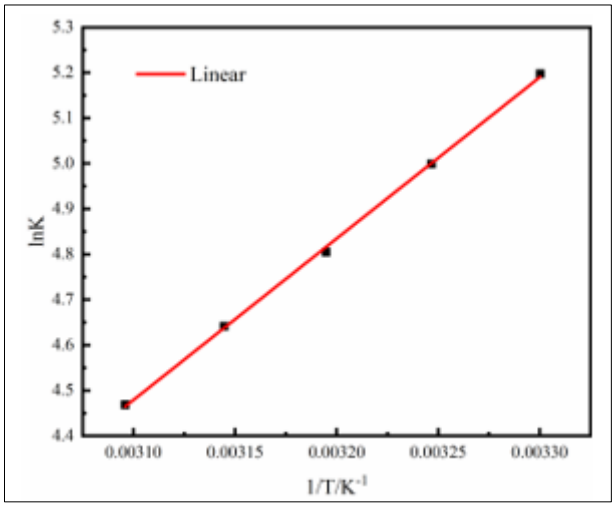

Figure 8. Linear fitting of ln K and 1/T

3.6 Kinetic calculation

3.6.1 External diffusion elimination

Outer diffusion refers to the process in which reactant molecules diffuse from the main body of the solution to the surface of the catalyst and are adsorbed on the surface of the catalyst. After the reaction occurs, the product desorbs and diffuses from the surface of the catalyst to the main body of the solution. For IFBR, when the volume flow rate reaches a certain value, the reaction rate basically no longer changes, indicating that the influence of the entire process of external diffusion on the reaction rate can basically be ignored [16], Based on the relevant literature analysis of our research group, When the liquid circulation flow in the IFBR unit is set at 40 mL/min, the influence of external diffusion can be eliminated [17].

3.6.2 Internal diffusion elimination

Internal diffusion refers to the diffusion of reactant molecules along the pores of the catalyst to the inside of the catalyst. After the reaction, the product diffuses from the pores of the catalyst to the surface of the catalyst. In an intensified fixed bed reactor, the reactant molecules diffuse from the main body of the solution to the surface of the catalyst, and then from the surface of the catalyst to the inside of the catalyst. At the same time, the molecules on the surface of the catalyst will react, that is to say, the driving force of internal diffusion. It is constantly decreasing. However, if the effective diffusion coefficient of each component in the solution is large, the concentration of the reactant in the catalyst pore is almost equal to the concentration at the pore opening, and the diameter of the catalyst is also a factor influencing internal diffusion. To evaluate the influence of internal diffusion, the Schiller modulus [18] and the effective coefficient of internal diffusion are used, and the expression is as follows:

$$\phi = \frac{R_p}{3}\sqrt{\frac{k}{D_e}} \tag{19}$$

In the formula, D_e can be estimated by formula (20) [19]:

$$D_e = \frac{\varepsilon_p \cdot D_A}{\tau} \tag{20}$$

The expression of D_A in the formula is [20]:

$$D_A = 7.4 \times 10^{-8} \frac{(\varphi M)^{1/2} T}{\mu V_b^{0.6}} \tag{21}$$

The formula for the effective coefficient of internal diffusion is:

$$\eta = \frac{1}{\phi}\left[\frac{1}{\tan(3\phi)} - \frac{1}{3\phi}\right] \tag{22}$$

Among them, τ can be represented by $1/\varepsilon_P$[21], and the value of ε_p/τ is generally between 0.25-0.5 [18,22]. When the Schiller modulus $\phi < 0.4$ and the effective coefficient of internal diffusion η tends to 1, the influence of internal diffusion can basically be ignored [23]. As shown in Table 5, within the experimental temperature range, the calculated η value tends to 1, indicating that NKC-9 can be ignored as the internal diffusion of the reaction catalyst.

Table 5. Thiele moduli and internal diffusion efficiency coefficient

T/K	303	308	313	318	323
ϕ	0.024	0.031	0.039	0.045	0.053
η	1.000	0.999	0.999	0.998	0.998

3.6.3 Kinetic model

Pseudo-homogeneous model (PH model) [24-28], Eley-Rideal (ER) model [29-31], Langmuir-Hinshelwood-Hougen-Watson (LHHW) model [32-36] is widely used in resin-catalyzed reactions System. In IFBR, the NKC-9 catalyst particles can be regarded as acid sites. The reaction is analogous

to a pseudo-homogeneous reaction system. Therefore, the PH model is used to fit the reaction. The reaction equation of camphene and acetic acid is as follows:

$$Cam + AA \underset{k_r}{\overset{k_f}{\rightleftharpoons}} IA$$

In the formula, k_f represents the positive reaction rate constant, k_r represents the reverse reaction rate constant, Cam represents camphene, AA represents acetic acid, and IA represents isobornyl acetate.

The reaction rate equation derived from the PH model is as follows:

$$\begin{aligned} \mathrm{r} = -\frac{da_{Cam}}{dt} &= -\frac{dx_{Cam}\gamma_{Cam}}{dt} = -\frac{dx^0_{Cam}\gamma_{Cam}(1-X)}{dt} \\ &= M_{cat}\left(k_f a_{Cam} a_{AA} - k_r a_{IA}\right) \\ &= M_{cat}\left(k_f a_{Cam} a_{AA} - \frac{1}{K} a_{IA}\right) \end{aligned} \quad (23)$$

Equilibrium constant $\mathrm{K} = k_f/k_r$, Mcat represents the mass of catalyst per unit volume of solution. Substituting the experimental data into the above formula, using 1Stopt software for simulation calculation, the simulation solution method uses the fourth-order Runge-Kutta method, and the objective function is expressed by the minimum residual square sum of the experimental value of camphene conversion and the calculated value. The expression is as follows:

$$\mathrm{SRS} = \sum(x_{exp} - x_{cal})^2 \quad (24)$$

In the formula, SRS represents the minimum residual sum of squares; x represents the conversion rate of camphene at each time point, x_{exp} represents the actual value measured by the experiment, x_{cal} represents the theoretical calculation value.

The Arrhenius equation is used to describe the relationship between the reaction rate constant and temperature, and its expression is:

$$\mathrm{k} = k_0 \exp\left(-\frac{E_a}{RT}\right) \quad (25)$$

Taking the logarithm of both sides can be expressed as:

$$\ln\mathrm{k} = \ln k_0 - \frac{E_a}{RT} \quad (26)$$

In the formula, k_0 is the pre-factor, and E_a is the activation energy. According to the above expressions, plot $\ln k_f$ and $\ln k_r$ versus 1/T, and calculate the pre-explicit factor k_0 and activation energy E_a according to the slope and intercept of the straight line, as shown in Figure 9. Through the 1Stopt software fitting, the forward and reverse reaction rate constants of camphene and acetic acid at different temperatures can be obtained. The results are shown in Table 6.

Table 6. The rate constant of reaction at different temperatures

T/K	303	308	313	318	323
$k_f(mol\cdot(g\cdot h)^{-1})$	0.224	0.361	0.515	0.618	0.862
$k_r \times 10^3(mol\cdot(g\cdot h)^{-1})$	1.239	2.435	4.216	5.961	9.886

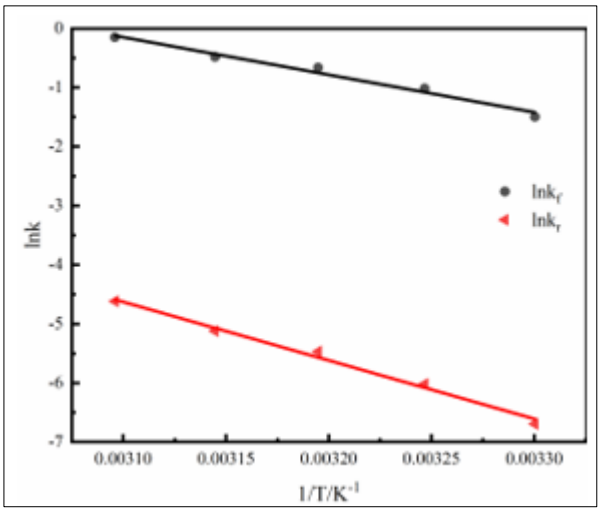

Figure 9. Linear fitting of lnK and 1/T

Through the linear fitting of lnk to 1/T, the rate constant of the forward and reverse reaction and the activation energy of the reaction can be obtained from the slope and intercept, as shown in Table 7.

Table 7. Kinetic parameters of PH model

	$k_0(mol \cdot (g \cdot h)^{-1})$	$E_a(kJ \cdot mol^{-1})$
Positive reaction	3.01 x 108	52.75
Reverse reaction	1.84 x 1011	81.99

$$k_f = 3.01 \times 10^8 \exp\left(-\frac{5.28 \times 10^4}{RT}\right)$$

$$k_r = 1.84 \times 10^{11} \exp\left(-\frac{8.20 \times 10^4}{RT}\right)$$

As shown in Figure 10, the comparison between the calculated value obtained by the pseudo-homogeneous model (PH model) and the experimental value shows that the two are in good agreement, indicating that NKC-9 is used as a catalyst to catalyze camphene and acetic acid in the IFBR. The kinetics of the esterification reaction can be expressed by a pseudo-homogeneous model.

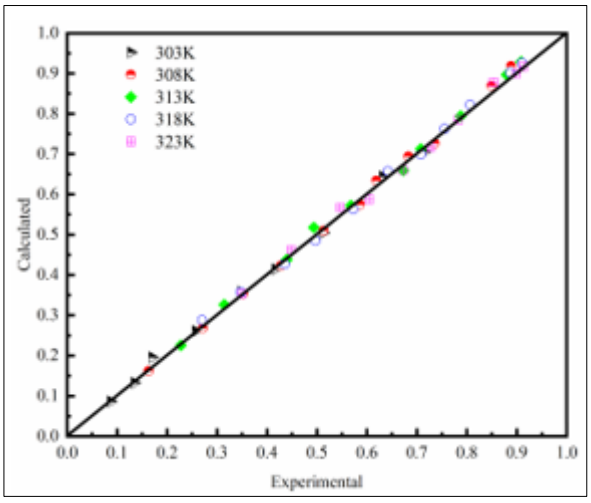

Figure 10. Comparison of experimental and calculated values of camphene conversion at different temperatures

4.Conclusions

The cation exchange resin NKC-9 was selected as the catalyst for the esterification reaction of camphene, and the influence of factors such as the amount of catalyst, the initial molar ratio of raw materials, and the reaction temperature on the esterification process of camphene and acetic acid was investigated and optimized process parameters. The final optimized reaction conditions are that the

catalyst loading is 15wt%, the initial molar ratio of raw materials is 1:1.5, and the reaction temperature is 308K. The recycling of the catalyst has industrial application value.

Using the UNIFAC group contribution method to calibrate the thermodynamic parameters, the equilibrium constant of the reaction based on the activity of camphene and acetic acid at 303-323K is calculated, and the enthalpy change $\Delta_r H^0$ of the reaction is -29.54kJ/mol, the entropy Change $\Delta_r S^0$ to -54.35J/(mol·K), Gibbs free energy $\Delta_r G^0$ to -13.55kJ/mol.

The pseudo-homogeneous model (PH model) was used to study the reaction kinetics, and the kinetic equation was obtained:

$$\mathrm{r} = -\frac{da_{Cam}}{dt} = M_{cat}(k_f a_{Cam} a_A - k_r a_{IA})$$

among them: $k_f = 3.01 \times 10^8 \exp\left(-\frac{5.28\times10^4}{RT}\right)$, $k_r = 1.84 \times 10^{11} \exp\left(-\frac{8.20\times10^4}{RT}\right)$.

The data obtained provides guidance for the industrial production of isobornyl acetate in a fixed bed reactor.

Nomenclature

γ_i – Component activity coefficient
$\gamma_i^{(c)}$ – Combined partial activity coefficient
$\gamma_i^{(R)}$ – Remaining part activity coefficient
θ_i – i component area fraction
ϕ_i –i component volume fraction
r_i – i component volume fraction
q_i – i component area fraction
Γ_k – Residual activity coefficient of k group in solution
$\Gamma_k^{(i)}$ – Residual activity coefficient of k group in pure component
$\hat{\theta}_m$ – Area fraction of group m in solution
$\hat{\theta}_m^{(i)}$ –Area fraction of group m in component i
$\hat{X}_m$ – Fraction of m-type groups in solution
$\hat{X}_m^{(i)}$ –Fraction of m-type groups in component i
a_{mn} – Group interaction parameters
a_{Cam} – Activity of Camphene, mol/L
a_{AA} – Activity of Acetic acid, mol/L
a_{IA} – Activity of isobornyl acetate, mol/L
D_A – Diffusion coefficient at infinite dilution, cm^2/s
D_e – Effective diffusion coefficient, cm^2/s
E_a – Activation ability, KJ/mol
k_f – Positive reaction rate constant, mol/(g·min)
k_r – Reverse reaction rate constant, mol/(g·min)
k_0 – Pre-reference factor, mol/(g·min)
M_{cat} – Catalyst mass per unit volume, g/L
R_p – Average catalyst particle size, mm
w/w – Catalyst mass/total mass of liquid materials
V_b – Molar volume of solution, cm^3/mol
x_{cal} – Calculated value of camphene conversion
x_{exp} – Experimental value of camphene conversion rate
φ – Association factor
μ – Viscosity, mPa·s
ε_p – Porosity
τ – Tortuosity factor
$\Delta_r G^0$ – Gibbs Free Energy, kJ/mol
$\Delta_r H^0$ – Reaction enthalpy change, kJ/mol
$\Delta_r S^0$ – Reaction entropy change, kJ/mol

Acknowledgement. We gratefully acknowledge the grants from the National Key R&D Program of China (No. 2018YFB0604600-05).

References

1.GU Y C, CAO J R, WU Z B, ZHANG M, SUN W. Main Factors Affecting the Esterification of Camphene with Lower Aliphatic Acid and Synthesis of Isobornyl Carboxylate[J]. Flavour Fragrance Cosmetics, 2013(S1): 60-62.
2.DIJS I J, VAN OCHTEN H L, DER HEIJDEN A J, et al. The catalytic performance of sulphonated cross-linked polystyrene beads in the formation of isobornyl acetate [J]. Applied Catalysis A-general, 2003, 241(1): 185-203.
3.MA W L. Isobornyl acetate was prepared from camphene in fixed bed with D72 resin[J]. Chemistry & Industry of Forest Products, 1989(01): 18-26.
4.DE MEIRELES A L, ROCHA K A, KOZHEVNIKOV I V, et al. Esterification of camphene over heterogeneous heteropoly acid catalysts: synthesis of isobornyl carboxylates[J]. Applied Catalysis A-general, 2011: 82-86.
5.YANG Y X, LI X K, WANG T, LEI Z B. Synthesis of Isobornyl Acetate with Solid Acid Catalyst SO42-/TiO_2 Supported by Phosphotungstic acid[J]. Shandong Chemical Industry, 2017, 46(24): 12-14.
6.CUI J T, YANG Y Z, LIANG X H, ZHAO Z D, HUANG J L. Synthesis of Isobornyl Acetate from Camphene Isomeric Esterification Catalyzed by Lewis Acids[J]. Chemistry and Industry of Forest Products, 2018, 38(01): 110-114.
7. LIU Y, LIU J, YAN H, et al. Kinetic Study on Esterification of Acetic Acid with Isopropyl Alcohol Catalyzed by Ion Exchange Resin[J]. Acs Omega, 2019.
8. HE X, XU R, WANG Y, et al. Methoxylation of dihydromyrcene in an intensified fixed bed reactor[J]. Chemical Engineering Research & Design, 2017: 254-262.
9. YANG G, CHEN S, LI X, et al. Study on Methyl Esterification of Salicylic Acid Using an Intensified Fixed Bed Reactor[J]. International Journal of Chemical Reactor Engineering, 2019.
10. CHEN S, WANG S, ZHOU Z, et al. Study on the Alkoxylation of Dihydromyrcene over Cation Exchange Resins[J]. Industrial & Engineering Chemistry Research, 2019, 58(27).
11. NIE H, XU R, ZHANG F, et al. Thermodynamic and kinetic studies on alkoxylation of camphene over cation exchange resin catalysts[J]. Aiche Journal, 2015, 61(6): 1925-1932.
12. RAN R, LI J, WANG G, et al. Esterification of Methacrylic Acid with Methanol: Process Optimization, Kinetic Modeling, and Reactive Distillation[J]. Industrial & Engineering Chemistry Research, 2019, 58(6): 2135-2145.
13. HE, X.; XU, R.; WANG, Y.; ZHANG, F.; LEI, Y.; ZHOU, Z.; ZHANG, Z. Methoxylation of dihydromyrcene in an intensified fixed bed reactor. Chem. Eng. Res. Des. 2017, 122, 254−262.
14.DONG X F, FANG L G, CHEN L. Principle to Estimate the Physical Properties and Computer Calculation[M]. Chemical Industry Press, 2006.
15. DONG Y, ZHU R, GUO Y, et al. A United Chemical Thermodynamic Model: COSMO-UNIFAC[J]. Industrial & Engineering Chemistry Research, 2018.
16. FOGLER H S. Elements of chemical reaction engineering[J]. Chemical Engineering Science, 1987, 42(10):2493-0.
17.CHEN L, LIU Y, CAO Z, et al. Thermodynamic and Kinetic Study on the Catalysis of Isoamyl Acetate by a Cation-Exchange Resin in an Intensified Fixed-Bed Reactor [J]. ACS Omega, 2020,
18. ZHANG Y, MA L, YANG J, et al. Kinetics of esterification of lactic acid with ethanol catalyzed by cation-exchange resins[J]. Reactive & Functional Polymers, 2004, 61(1): 101-114.
19. SANTHANAKRISHNAN A, SHANNON A, PEEREBOOM L, et al. Kinetics of Mixed Ethanol/n-Butanol Esterification of Butyric Acid with Amberlyst 70 and p-Toluene Sulfonic Acid[J]. Industrial & Engineering Chemistry Research, 2013, 52(5): 1845-1853.
20. POLING B E, PRAUSNITZ J M, O'CONNELL J P. The properties of gases and liquids; 5th ed, Mcgraw-hill: New York, 2001.

21. WAKAO N, SMITH J M. Diffusion in catalyst pellets[J]. Chemical Engineering Science, 1962, 17(11): 825-834.
22. LILJA J, AUMO J, SALMI T, et al. Kinetics of esterification of propanoic acid with methanol over a fibrous polymer-supported sulphonic acid catalyst[J]. Applied Catalysis A-general, 2002, 228(1): 253-267.
23.GUO K, TANG X H, ZHOU X M. Chemical reaction engineering [M]. 2nd edition. Beijing Chemical Industry Press, 2007.
24. YANG G, LIU Y, ZHOU Z, et al. Kinetic study of the direct hydration of turpentine[J]. Chemical Engineering Journal, 2011, 168(1): 351-358.
25. HE X, XU R, ZHANG L, et al. Alkoxylation of camphene catalyzed by cation exchange resins[J]. Chemical Engineering Research & Design, 2016: 60-68.
26. yang, g, wu, p, zhou, z, he, x, meng, w, & zhang, z. (2012). Direct Hydration of β-Caryophyllene. Industrial & Engineering Chemistry Research, 51(49), 15864–15871.
27. DELGADO P, SANZ M T, BELTRAN S, et al. Kinetic study for esterification of lactic acid with ethanol and hydrolysis of ethyl lactate using an ion-exchange resin catalyst[J]. Chemical Engineering Journal, 2007, 126(2): 111-118.
28. GANGADWALA J, MANKAR S, MAHAJANI S M, et al. Esterification of Acetic Acid with Butanol in the Presence of Ion-Exchange Resins as Catalysts[J]. Industrial & Engineering Chemistry Research, 2003, 42(10): 2146-2155.
29. ESTEBAN J, LADERO M, GARCIAOCHOA F, et al. Kinetic modelling of the solventless synthesis of solketal with a sulphonic ion exchange resin[J]. Chemical Engineering Journal, 2015: 194-202.
30. KHUDSANGE C R, WASEWAR K L. Kinetic study of liquid phase esterification of lactic acid with n-amyl alcohol catalyzed by cation exchange resins: experimental and statistical modeling[J]. Reaction Kinetics, Mechanisms and Catalysis, 2018, 125(2): 535-554.
31.QIAN J, QIU M, ZENG Z, et al. Cation-Exchange Resin Catalyzed Ketalization Reaction of Cyclohexanone with 1,4-Butanediol: Thermodynamics and Kinetics[J]. Industrial & Engineering Chemistry Research, 2018, 57(14): 4841-4847.
32.CAIADO M, MACHADO A, SANTOS R N, et al. Alkoxylation of camphene over silica-occluded tungstophosphoric acid[J]. Applied Catalysis A-general, 2013: 36-42.
33. RAHAMAN M, GRACA N S, PEREIRA C S, et al. Thermodynamic and kinetic studies for synthesis of the acetal (1,1-diethoxybutane) catalyzed by Amberlyst 47 ion-exchange resin[J]. Chemical Engineering Journal, 2015: 258-267.
34. AKYALCIN S. Kinetic Study of the Formation of Isopropyl Alcohol by Transesterification of Isopropyl Acetate with Methanol in the Presence of Heterogeneous Catalyst[J]. Industrial & Engineering Chemistry Research, 2014, 53(23): 9631-9637.
35. OSORIOVIANA W, DUQUEBERNAL M, FONTALVO J, et al. Kinetic study on the catalytic esterification of acetic acid with isoamyl alcohol over Amberlite IR-120[J]. Chemical Engineering Science, 2013: 755-763.
36. CHIN S Y, AHMAD M A, KAMARUZAMAN M R, et al. Kinetic studies of the esterification of pure and dilute acrylic acid with 2-ethyl hexanol catalysed by Amberlyst 15[J]. Chemical Engineering Science, 2015: 116-125

Manuscript received: 21.10.2020